Seasonal variations in the Amazon plume-related atmospheric carbon sink

S. R. Cooley,[1] V. J. Coles,[2] A. Subramaniam,[3] and P. L. Yager[1]

Received 12 September 2006; revised 23 March 2007; accepted 29 May 2007; published 28 August 2007.

[1] The Amazon River plume is a highly seasonal feature that can reach more than 3000 km across the tropical Atlantic Ocean, and cover ~2 million km^2. Ship observations show that its seasonal presence significantly reduces sea surface salinity and inorganic carbon. In the western tropical North Atlantic during April–May 2003, plume-influenced stations exhibited surface DIC concentrations lowered by as much as 563 μmol C kg^{-1} (~28%) and pCO_2 as low as 201 μatm. We combine our data with other data sets to understand the annual uptake and seasonal variability of the plume-related CO_2 sink. Using flux estimates from all seasons with monthly plume areas determined by satellite, we calculate the annual carbon uptake by the outer plume alone ($28 < S < 35$) to be 15 ± 6 TgC yr^{-1}. Diazotroph-supported net community production enhanced the air-sea CO_2 disequilibrium by 100x and reversed the typical CO_2 outgassing from the tropical North Atlantic. The carbon sink in the Amazon plume depends on climate-sensitive conditions that control river hydrology, CO_2 solubility, and gas exchange.

Citation: Cooley, S. R., V. J. Coles, A. Subramaniam, and P. L. Yager (2007), Seasonal variations in the Amazon plume-related atmospheric carbon sink, *Global Biogeochem. Cycles*, *21*, GB3014, doi:10.1029/2006GB002831.

1. Introduction

[2] The Amazon River generates an offshore plume that covers ~2×10^6 km^2 of the western tropical North Atlantic Ocean (WTNA) each summer with a thin (5–10 m) layer of low-inorganic-carbon, and low-salinity (S) water [*Lentz and Limeburner*, 1995; *Körtzinger*, 2003; *Ternon et al.*, 2000; *Smith and DeMaster*, 1996; *DeMaster and Pope*, 1996]. Effects of the plume on pCO_2 may reach as far as 3000 km east to 25°W during peak autumn surface flow of the North Equatorial Countercurrent [*Lefevre et al.*, 1998; *Bakker et al.*, 1999]. As in the Congo River plume [*Bakker et al.*, 1999], net community production (NCP) enhances the mixing-driven air-sea CO_2 gradient [*Cooley and Yager*, 2006], and the Amazon plume absorbs ~5.8 gC m^{-2} yr^{-1} atmospheric CO_2 (0.014 Pg C yr^{-}1 over $15 < S < 35$ and 2×10^6 km^2 [*Körtzinger*, 2003]). In contrast, the tropical Atlantic at large releases approximately 8.2 gC m^{-2} yr^{-1} between 20°N and 20°S (for a total of 0.15 PgC yr^{-1} [*Takahashi et al.*, 2002]) owing to solubility-driven CO_2 loss in excess of biological uptake [*Goyet et al.*, 1998; *Lee et al.*, 1997; *Takahashi et al.*, 1997, 2002; *Sarmiento et al.*, 1995]. The seasonal extension of the Amazon plume thus drives WTNA temporal dissolved inorganic carbon (DIC) variability by reversing the air-sea CO_2 flux over a large region.

[3] Previous estimates of annual plume carbon uptake [*Körtzinger*, 2003; *Ternon et al.*, 2000] are based on DIC-S relationships from one or two offshore plume transects, spatially extrapolated using ship-based, monthly sea surface salinity (SSS) climatologies. Until now, limited spatial and temporal coverage has hampered assessment of Amazon plume DIC variability. In this study, we improve current coverage by applying a satellite-based model of plume S to four published data sets and one new data set. We investigate temporal changes in river supply and offshore processes to explain observed seasonality. This work extends our mechanistic understanding of the tropical Atlantic CO_2 sink, which will assist future predictions of sink behavior under changing climate conditions.

[4] Biological, geochemical, and physical processes regulate DIC movement into and within the Amazon plume. Total alkalinity (TA), a carbonate system parameter, appears to be a nearly conservative tracer of both Andean water within the river main stem [*Devol et al.*, 1995, and references therein] and Amazon water in the offshore plume [*Ternon et al.*, 2000; *Cooley and Yager*, 2006]. Andean runoff provides most of the Amazon River's alkalinity as bicarbonate, which is diluted downstream by Amazon tributaries draining weathered, low-carbonate soils [*Gibbs*, 1972; *Stallard and Edmond*, 1983; *Richey et al.*, 1991; *Devol and Hedges*, 2001; *Marengo et al.*, 2001; *Grimm*, 2003]. Bicarbonate is the main component of TA in most natural waters whose pH is below 7 [*Stumm and Morgan*, 1996]. TA peaks upriver in March (~700 μmol kg^{-1} at Marchanteria, 1500 km from the river mouth [*Devol et al.*, 1995; *Devol and Hedges*, 2001]), and ranges between 360

[1]School of Marine Programs, University of Georgia, Athens, Georgia, USA.
[2]University of Maryland Center for Environmental Science, Horn Point Laboratory, Cambridge, Maryland, USA.
[3]Lamont-Doherty Earth Observatory, Palisades, New York, USA.

0886-6236/07/2006GB002831

and 600 μmol kg^{-1} near the river midpoint (at Óbidos, 800 km from the mouth [*Devol and Hedges*, 2001]). Although TA at the Amazon mouth has not been measured in a time series, monthly bicarbonate levels at Macapá averaged 370 μmol kg^{-1} from April 1963 to May 1964, and ranged between 247 and 551 μmol kg^{-1} [*Gibbs*, 1972]. One quarter to one third of total Amazon discharge enters downstream of Óbidos from low-TA lowland rivers such as the Tapajós (TA = 82 μmol L^{-1} [*Stallard and Edmond*, 1983]), Xingu (TA = 176 μmol L^{-1} [*Stallard and Edmond*, 1983]), and Tocantins. Main stem TA decreases correspondingly: In June 1976, TA was 323 μmol L^{-1} near Óbidos, and 308 μmol L^{-1} just west of Marajó Island, near the mouth [*Stallard and Edmond*, 1983]. In June 1977, TA was 386 μmol L^{-1} at Óbidos and 359 μmol L^{-1} just above the Xingu confluence [*Stallard and Edmond*, 1983].

[5] Total alkalinity can be altered nonconservatively by biological activity [*Morel*, 1983; *Stumm and Morgan*, 1996]. Photosynthesis and respiration alone do not alter TA, but other biogeochemical changes can. Nutrient uptake or remineralization causes small TA changes, and some plankton lower TA by secreting carbonate tests. Assuming Redfield stoichiometry and a soft-to-hard tissue production ratio of 4:1, biological activity changes TA by 28% of the net DIC change [*Broecker and Peng*, 1982]. If the 4:1 ratio increases (up to 40:1 in some regions [*Pätsch et al.*, 2002; *Hood et al.*, 2006]), then the biologically associated TA change would be a much lower percentage of the DIC change. Higher ratios are expected in regions dominated by diatom blooms [*Rixen et al.*, 2006].

[6] Dissolved inorganic carbon is not expected to act conservatively along the mountain-ocean mixing gradient [*Devol and Hedges*, 2001; *DeMaster and Aller*, 2001; *Ternon et al.*, 2000; *Cooley and Yager*, 2006]. Net remineralization of riverine organic matter releases CO_2 to the atmosphere [*Devol et al.*, 1987; *Richey et al.*, 2002; *Mayorga et al.*, 2005] until turbidity settles in the early plume (S = 0–3 [*DeMaster et al.*, 1996; *Edmond et al.*, 1981] Plume nutrients support net primary production offshore [*Smith and DeMaster*, 1996; *DeMaster and Pope*, 1996], which lowers pCO_2 below atmospheric levels and leads to CO_2 uptake [*Ternon et al.*, 2000; *Körtzinger*, 2003; *Cooley and Yager*, 2006]. Although the carbonate system near the mouth is not well studied [*Körtzinger*, 2003], the DIC level in the main stem below Óbidos (at Ituqui) is about 350 μmol kg^{-1} (estimated from TA = 295, pH = 6.64 [*Stallard and Edmond*, 1983]), and values at the river mouth are low (363 μmol kg^{-1} in November 1991 [*Druffel et al.*, 2005]) compared to the ocean. With relatively few data at the mouth and none reporting more than one carbonate system parameter, analyses offshore [*Ternon et al.*, 2000, and references therein; *Körtzinger*, 2003; *Cooley and Yager*, 2006] have assumed that DIC at the mouth co-occurs with TA in a fixed ratio (similar to that observed upriver by *Devol et al.* [1995]) and varies little. Until more is known about the carbonate system at the mouth, we must assume that seasonal changes in riverine DIC follow TA changes, which are small compared to biological production and air-sea CO_2 transfer in the plume.

[7] We report a new data set for WTNA surface mixed layer DIC, TA, and underway pCO_2 measured during spring 2003 and use this data with historical data from the WTNA [*Ternon et al.*, 2000; *Körtzinger*, 2003; *Cooley and Yager*, 2006] and Amazon main stem [*Devol et al.*, 1995] to examine seasonality in the Amazon plume-associated CO_2 sink. We quantify potential seasonality in riverine supply by modeling TA at the river mouth with two independent methods. We also quantify the biological impact on plume DIC over four seasons and then apply climatological control to calculate seasonal gas exchange. Combining seasonal CO_2 flux estimates with satellite-based plume areas provides an estimate of the total annual plume CO_2 uptake that includes observed variability.

2. Methods

2.1. Sample Collection and Analysis

[8] The spring 2003 (Sp03) samples were collected during daily stations aboard the R/V *Seward Johnson I* on the eighth MANTRA/PIRANA ("MP8") cruise (6°N–13°N, 48°W–58°W; Figure 1 and Table 1). Water samples for DIC and TA analysis were collected between 1 and 1000 m and stored according to standard protocols [*Department of Energy*, 1997; *Cooley and Yager*, 2006]. In addition, a single sample of Amazon surface water was collected from a small boat near Macapá, Brazil (0°N, 51°W; Figure 1) on 25 March 2002 using a pole sampler. The sample was not fixed but was sealed tightly and shipped to Georgia, where it was refrigerated in the dark until analysis in 2005.

[9] During the cruise, surface ocean pCO_2 was measured continuously using an automated underway analyzer plumbed into the ship's uncontaminated seawater line. The system's primary components included a 10 L showerhead-type seawater equilibrator [*Bates et al.*, 1998; *Sweeney et al.*, 2000; *Takahashi et al.*, 1997] and an infrared CO_2 detector (LI-6262, Li-Cor, Lincoln, Nebraska). Seawater flow of 8 L min^{-1} produced a system e-folding time of 35 minutes (S. Cooley, unpublished data, 2006). Measurements were automatically calibrated at least hourly against five CO_2-N_2 gas mixtures containing 0–510.85 ppm CO_2 (certified by the National Oceanographic and Atmospheric Administration Climate Monitoring and Diagnostics Laboratory, NOAA CMDL, Boulder, Colorado, USA). Instrument accuracy was ±1 μatm. pCO_2 was calculated at in situ temperature [*Takahashi et al.*, 1993]. A Lanczos filter [*Duchon*, 1979] (100 weights, cutoff frequency = 9.3 × 10^{-5} Hz) was used to remove occasional brief high-pCO_2 excursions related to short interruptions in the ship's seawater supply during high seas.

[10] DIC measurements were performed on a SOMMA [*Johnson et al.*, 1993; *Cooley and Yager*, 2006] connected to a CO_2 coulometer (UIC, model 5011) and equipped with a Sea-Bird conductivity cell (SBE-4). Salinity (S, practical salinity scale, unitless) was calculated on the basis of cell calibration to IAPSO standards. Precision based on analysis of replicate standards or replicate samples [*Department of Energy*, 1997] was ±0.51 and ±1.58 μmol C kg SW^{-1}, respectively.

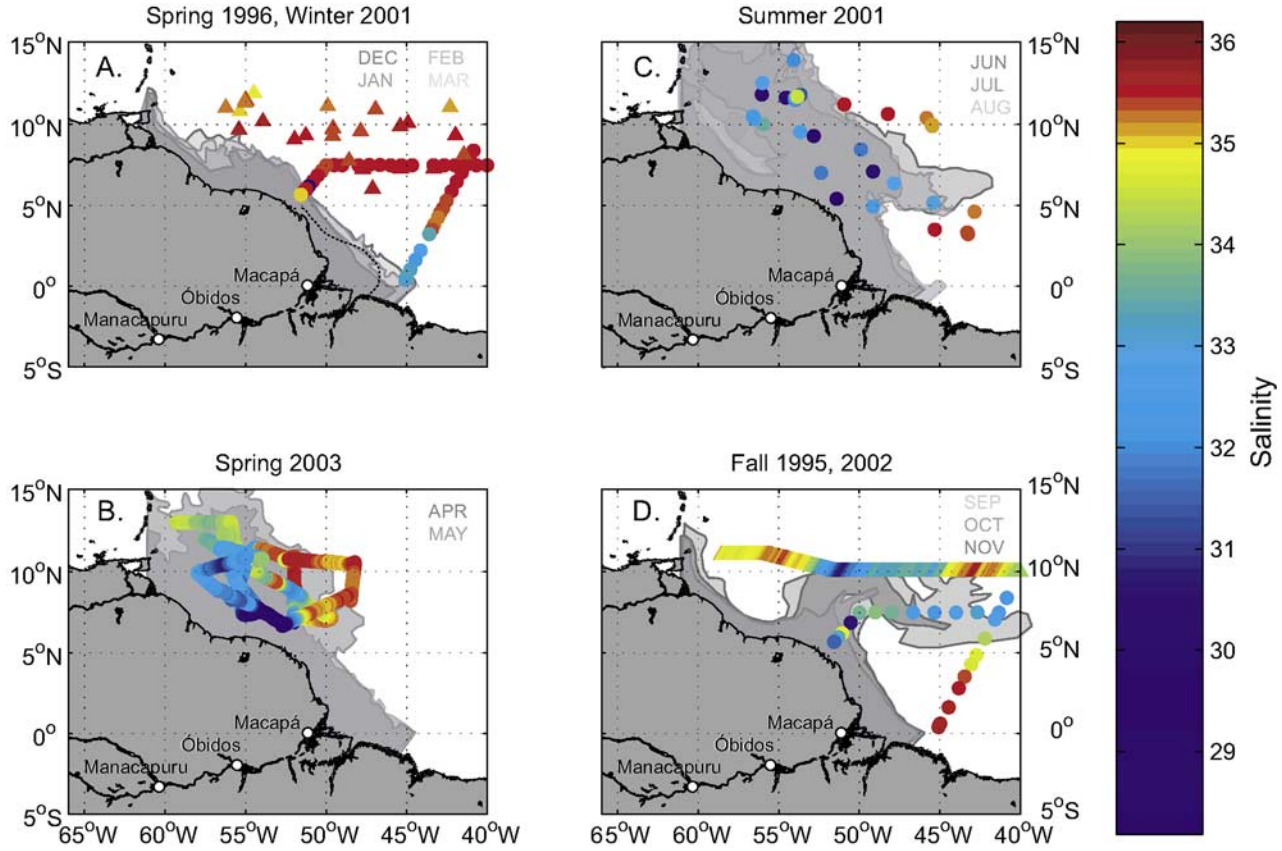

Figure 1. Sea surface salinity for each data set superimposed over monthly Amazon plume (S < 35) areas derived from satellite data. (a) Spring 1996 data [*Ternon et al.*, 2000] are marked with circles, and winter 2001 (W01) data [*Cooley and Yager*, 2006] are marked with triangles. The dashed line in Figure 1a indicates the possible location of the plume during periods of northerly winds in February and March [after *Geyer et al.*, 1996]. (b) Spring 2003 (this paper). (c) Summer 2001 [*Cooley and Yager*, 2006]. (d) Fall 1995 data [*Ternon et al.*, 2000] are marked with circles, and fall 2002 (F02) [*Körtzinger*, 2003] data are marked with triangles.

[11] TA was measured using a programmable open-cell potentiometric titration system [*Dickson et al.*, 2003; *Bates et al.*, 1996; *Cooley and Yager*, 2006]. Precision based on replicate standards and replicate samples [*Department of Energy*, 1997] was ±1.93 or ±1.66 μmol kg^{-1}, respectively.

[12] The Macapá sample was centrifuged at 8500 rpm for 20 minutes to remove the larger suspended sediment particles before chemical analysis. Salinity was determined using the SOMMA conductivity cell, and TA was measured as described above.

2.2. Historical Observational Data Sets

[13] WTNA DIC, TA, and pCO_2 from other seasons and years were also used for this study (Figure 1 and Table 1): fall 1995 (F95) and spring 1996 (Sp96) [*Ternon et al.*, 2000]; October–November 2002 [*Körtzinger*, 2003]; summer (Su01) and winter 2001 (W01) [*Cooley and Yager*, 2006]. Atmospheric pCO_2 at Ragged Point, Barbados was obtained from NOAA CMDL.

2.3. Data Analysis

2.3.1. Observational Data

[14] Following previous analyses [*Cooley and Yager*, 2006; *Lentz and Limeburner*, 1995; *Geyer et al.*, 1996; *Lentz*, 1995b], plume stations were identified by low surface salinities (<35) and shallow haloclines overlying oceanic-S water. Surface mixed layer (SML) depths used to select the plume-influenced data were calculated from CTD profiles using a density gradient criterion ($\Delta\rho/\Delta z > 0.01$ [*Brainerd and Gregg*, 1995]). The critical value throughout the analysis for statistical significance was $\alpha = 0.05$, and mean values are presented with their standard error unless otherwise noted.

[15] F95 and Sp96 TA reported by *Ternon et al.* [2000] were originally calculated from DIC and pH using the *U.N. Educational, Scientific and Cultural Organization* [1987] definition and the *Roy et al.* [1993] dissociation constants. To ensure consistency among data sets, we recalculated TA from measured DIC and pH [*Ternon et al.*, 2000] with CO2SYS [*Lewis and Wallace*, 1998], using the *Dickson*

Table 1. Data Used in This Analysis

Sample/Data Type	Name	Date	Citation, Source
		Offshore WTNA Inorganic Carbon Data	
DIC, TA, pCO_2	spring 2003 (Sp03) (MANTRA/PIRANA 8)	18 April to 22 May 2003	this paper, new data http://cdiac.ornl.gov/oceans/RepeatSections/MP_Cruises.html
TA, single value	spring 2002 (Sp02) (Macapá hand sample)	April 2002	this paper, new data
pCO_2	fall 2002 (F02) (Meteor 55)	13 October to 17 November 2002	*Körtzinger* [2003] A. Körtzinger (personal communication, 2005)
DIC, TA	summer 2001 (Su01) (MANTRA/PIRANA 3)	9 July to 19 August 2001	*Cooley and Yager* [2006], http://cdiac.ornl.gov/oceans/RepeatSections/MP_cruises.html
DIC, TA	winter 2001 (W01) (MANTRA/PIRANA 1)	January to February 2001	*Cooley and Yager* [2006], http://cdiac.ornl.gov/oceans/RepeatSections/MP_cruises.html
DIC, TA, fCO_2	spring 1996 (Sp96) (ETAMBOT II)	12 April to 16 May 1996	*Ternon et al.* [2000], www.ifremer.fr/sismer
DIC, TA, fCO_2	fall 1995 (F95) (ETAMBOT I)	9 September to 11 October 1995	*Ternon et al.* [2000], www.ifremer.fr/sismer
DIC, single value	November 1991 (Macapá sample)	November 1991	*Druffel et al.* [2005]
		Supplementary Carbon and Hydrologic Data	
Atmospheric pCO_2	Ragged Point, Barbados	1995–2003	www.cmdl.noaa.gov/ftpdata.html
River TA	Manacapuru TA (TA_{Man})	1982–1992	*Devol et al.* [1995]
Amazon discharge (see text)	Q_{SPdO}, Q_{Man}, Q_{Obi}	1968–2005	http://hidroweb.ana.gov.br
Monthly precip.	GPCP (NASA GPCP V2 Combined Precip. Data Set)	January 1979 to January 2004	*Huffman* [1997], http://precip.gsfc.nasa.gov
	CMAP (CPC Merged Analysis of Precipitation)	January 1979 to May 2005	*Xie and Arkin* [1997], www.cpc.ncep.noaa.gov
Monthly river discharge rates	Dai and Trenberth climatology	1 year	*Dai and Trenberth* [2002]
Gridded wind speed	SSM/I	1 January 1995 to 20 July 1999	*Atlas et al.* [1996] http://podaac-www.jpl.nasa.gov/
	QuikSCAT	21 July 1999 to 31 December 2005	*Atlas et al.* [1996] http://podaac-www.jpl.nasa.gov/

[1981] TA definition, carbonate dissociation constants of *Mehrbach et al.* [1973], refit by *Dickson and Millero* [1987] (valid for salinities 20–40), borate constants of *Dickson* [1990b], and KSO_4 dissociation constants of *Dickson* [1990a]. Our calculated fCO_2 data for F95 and Sp96, determined using recalculated TA and measured DIC in CO2SYS [*Lewis and Wallace*, 1998] (see below), compared well to measurements of fCO_2 by *Ternon et al.* [2000] (average difference = 0.8 ± 1.5 μatm). Subsequent analysis of 1995–1996 data used reported DIC, reported fCO_2 (converted to pCO_2 where appropriate), and recalculated TA.

2.3.2. Modeled Main Stem TA

[16] Estimated TA at the river mouth from 1991–2003 was modeled by predicting main stem TA at an upstream river gauging station (Manacapuru) based on Andean discharge, and propagating this TA signal downstream to the river mouth. Following the method of Devol et al. (1995), a multiple regression equation was developed to predict Manacapuru TA (1700 km inland, Figure 1) using measured Manacapuru TA from 1982–1992 [*Devol et al.*, 1995], daily Manacapuru discharge (Q_{Man}, Table 1), and percent Andean discharge (A%). Andean discharge to the Amazon has been defined as main stem discharge at Sao Paulo de Olivença (Q_{SPdO} [*Devol et al.*, 1995; *Quay et al.*, 1992; *Richey et al.*, 1990] (Table 1 and Figure 1)), making A% = $(Q_{SPdO}/Q_{Man})*100\%$.

[17] For the periods in 1991–2003 where Hidroweb records of Manacapuru discharge are not continuous (1991–1996, 2002–2003), we estimated Q_{Man} as a fraction of Óbidos discharge (Q_{Obi}, Table 1, continuous for 1969–2005). We calculated the daily ratio of Manacapuru discharge to Óbidos discharge ($M = Q_{Man}/Q_{Obi}$) when discharge records overlapped (June 1972 to December 1984, January 1996 to December 2001). Daily ratios from all 17 years were averaged into mean daily ratios (M_D), and Q_{Man} data missing from the Hidroweb record were filled with $Q_{Man,\ predicted} = M_D*Q_{Obi}$ (75% of Hidroweb Q_{Man} data was randomly selected to calculate M_D, and the remaining 25% was compared to $Q_{Man,\ predicted}$ to check prediction accuracy). Daily Manacapuru TA (TA_{Man}) was calculated for 1991–2003 with A%, the continuous Q_{Man}, and the multiple regression equation.

[18] To obtain river mouth TA, the Andean signal was diluted into the total river discharge at Macapá (location on Figure 1), assuming no lowland contributions to alkalinity. For each month of 1991–2003, mean TA_{Man} and Q_{Man} were calculated from daily values, and monthly TA at Macapá was predicted by the equation: $TA_{Macapá} = TA_{Man}*Q_{Man}/Q_{Total}$, where Q_{Total} is modeled monthly total Amazon discharge using precipitation data (see next paragraph). Monthly $TA_{Macapá}$ was further combined into an interannual climatology to show average seasonal variability. Error

associated with mean discharge and multiple regression equation-modeled TA was propagated throughout the dilution model by a Monte Carlo method [see *Yager et al.*, 1995].

2.3.3. Modeled Main Stem Discharge

[19] Previous Amazon hydrology studies [e.g., *Zeng*, 1999; *Labat et al.*, 2004] suggest that interannual and annual precipitation signals dominate river discharge data. To capture maximum interannual variation, total Amazon discharge was modeled by combining a seasonal discharge climatology [*Dai and Trenberth*, 2002] (based on streamflow coupled to a runoff database) with integrated precipitation over the watershed. Two climatologies based on monthly precipitation databases were used (GPCP and CMAP, Table 1). Precipitation was lagged and linearly correlated to the *Dai and Trenberth* [2002] climatology. Adjusted discharge was then calculated using the precipitation climatology and the linear relationship. The resulting two linear models coupling discharge and precipitation climatologies were applied to interannually varying precipitation data to estimate total Amazon discharge at the river mouth (Q_{tot}). For comparison, the Óbidos gauge was projected to the river mouth using a linear regression against the Amazon River mouth climatology. Data from the Óbidos gauging station obtained from SAGE Global River Discharge Database www.sage.wisc.edu/riverdata) were used to validate the model. As above, linear models were also constructed on the basis of the relation between interannually varying precipitation and Óbidos data projected to the river mouth.

2.3.4. Mixing Model: River End-Members and Biological DIC Drawdown

[20] A previously described conservative mixing model [*Cooley and Yager*, 2006] was used to determine the proportions of river water and seawater in each sample based on S. We used this information, non-plume-influenced seawater end-member TA (TA_s), and observed sample TA (TA_{obs}) to calculate the river end-member TA (TA_r). The mixing-modeled TA_r was then compared to discharge-modeled $TA_{Macapá}$.

[21] The mixing model was also used to calculate biological effects on DIC for all plume-influenced samples for which DIC and TA were available [*Cooley and Yager*, 2006]. W01 and fall 2002 (F02) data were not analyzed this way because W01 sampling did not encounter the river plume [*Cooley and Yager*, 2006], and the F02 published data set did not include DIC and TA. The model calculates expected DIC (DIC_{exp}) of each sample, which is the DIC value if conservative river-ocean mixing were the only influence. The difference between DIC_{exp} and measured DIC (DIC_{obs}) is attributed to biological activity and is ΔDIC_{bio}. Positive ΔDIC_{bio} values indicate net production, and negative values indicate net respiration. To avoid skewing the seasonal analysis, we only used data for outer plume water with salinities between 28 and 35, where all seasons had good coverage. Seawater end-members used in the mixing model were average values of pooled nonplume ($S > 35$) SML samples from all five cruises ($S_s = 36.04 \pm 0.22$, $TA_s = 2367 \pm 18$ μmol kg^{-1}, $DIC_s = 2014 \pm 19$ μmol kg^{-1}; mean ± s.d., n = 254). Error associated with average end-member values was propagated through the mixing model by a Monte Carlo method [see *Yager et al.*, 1995].

2.3.5. The pCO_2 and CO_2 Flux Estimates

[22] In situ pCO_2 (hereafter pCO_{2obs}) was calculated for W01 and Su01 [*Cooley and Yager*, 2006] from discrete surface DIC and TA values using CO2SYS [*Lewis and Wallace*, 1998]. Measured pCO_2 from other seasons and years (this study and *Ternon et al.* [2000]) was used in the rest of the analysis. In addition, the pCO_2 expected if conservative river-ocean mixing were the only influence on the system (pCO_{2mix}) was calculated for plume-influenced data sets using CO2SYS and measured temperature, S, nutrients, TA_{obs}, and DIC_{exp} output from the mixing model, with CO2SYS settings as described above.

[23] Air-sea fluxes into the Amazon plume were calculated for pCO_{2obs} and pCO_{2mix} to assess seasonal biological enhancement of the sink. Assuming pCO_{2obs} represents the combined effects of mixing plus biology, the difference between fluxes is attributed to biology. Both fluxes were calculated for each plume-influenced data set using solubility [*Weiss*, 1974], piston velocity (short-term wind formulation of *Wanninkhof and McGillis* [1999]), and the air-sea pCO_2 gradient ($\Delta pCO_2 = pCO_{2\ atm} - pCO_{2\ sea}$). Atmospheric pCO_2 was assumed to be 370 μatm, near the average value (368.4 ± 2.3 μatm, n = 10) of atmospheric values at Ragged Point, Barbados during the cruises. Winds [*Atlas et al.*, 1996] (Table 1) were averaged over space (4°N–13°N, 40°W–60°W) and time to yield mean daily wind speeds for the study region. Climatological daily winds for the WTNA were then determined using all 1995–2005 data. Standard deviations from averaging wind speeds were propagated through air-sea flux calculations and plume uptake estimates (below) by Monte Carlo as described above.

[24] We examined air-sea CO_2 fluxes and parameters influencing them (ΔDIC_{bio}, ΔpCO_{2obs}, ΔpCO_{2mix}, solubility, and climatological winds) for temporal or S-related trends. Plume-influenced data was grouped by cruise (Sp95, F96, Su01, Sp03) or by S (28–30, 30–32, 32–35). Equality of group variances was tested with Bartlett's test for homogeneity of variances [*Sokal and Rohlf*, 2000]. When group variances were equal (see Table 2), group means were compared using an ANOVA. When group variances were unequal, group data distributions were compared with the more appropriate nonparametric Kruskal-Wallis test for differences in location of ranked data [*Sokal and Rohlf*, 2000].

[25] Outer plume surface area was obtained from SeaWiFS satellite derived maps of diffuse attenuation coefficient at 490 nm (K_{490}) using a S-K_{490} relationship [*Del Vecchio and Subramaniam*, 2004] (also A. Subramaniam et al., Amazon River enhances diazotrophy and carbon sequestration in the tropical North Atlantic Ocean, submitted to *Nature*, 2007, hereinafter referred to as Subramaniam et al., submitted manuscript, 2007). Briefly, monthly climatological binned 9-km level 3 data of K_{490} for the WTNA were extracted on the basis of the relationship between in situ measurements of K_{490} and S [*Del Vecchio and Subramaniam*, 2004]: $K_{490} = 0.021(\pm 0.002)*S + 0.768(\pm 0.057)$, (mean ± s.d., $r^2 = 0.93$). This formulation is only valid for $28 < S < 35$ in the Amazon plume-

Table 2. Testing for Differences in Mean (ANOVA) or Data Distributions (Kruskal-Wallis; KW) Between Cruises or Salinity Groups (28–30, 30–32, 32–35) for Parameters Related to Air-Sea CO_2 Transfer[a]

	Cruise Groups			Salinity Groups		
	Variances	ANOVA P Value	KW P Value	Variances	ANOVA P Value	KW P Value
			All Data			
ΔDIC_{bio}	≠		**0.0004**	=	0.9688	0.9231
Solubility	≠		**<0.0001**	=	0.8421	0.9062
ΔpCO_{2obs}	≠		**0.0005**	=	0.2377	0.0515
ΔpCO_{2mix}	=	**0.0263**	**0.0428**	=	**0.0002**	**0.0009**
$\Delta\Delta pCO_{2bio}$	≠		**0.0007**	≠		0.9540
Wind speed	=	**<0.0001**	**<0.0001**	=	0.5611	0.7838
$Flux_{obs}$	≠		**0.0001**	=	0.8180	0.3212
$Flux_{mix}$	=	**0.0371**	0.0657	=	**0.0007**	**0.0038**
$\Delta Flux_{bio}$	≠		**0.0016**	≠		0.9098
			Sp03, Su01, F95			
ΔDIC_{bio}	=	0.1580	0.0470	=	0.9720	0.9282
Solubility	≠		**<0.0001**	=	0.9140	0.9249
ΔpCO_{2obs}	=	0.3340	0.2598	=	0.4642	0.1212
ΔpCO_{2mix}	=	**0.0179**	**0.0315**	=	**0.0004**	**0.0012**
$\Delta\Delta pCO_{2bio}$	=	0.6651	0.4402	≠		0.9493
Wind speed	=	**<0.0001**	**<0.0001**	=	0.6373	0.8644
$Flux_{obs}$	≠		**0.0119**	=	0.9398	0.6171
$Flux_{mix}$	=	**0.0394**	**0.0431**	=	**0.0010**	**0.0044**
$\Delta Flux_{bio}$	=	0.8310	0.2533	≠		0.6482

[a]Top part of table includes all four cruises. Bottom part of table tests for differences between spring 2003 (Sp03), summer 2001 (Su01), and fall 1995 (F95) only. Significant effects at the >95% confidence level are indicated in boldface.

influenced WTNA. High CDOM levels associated with Orinoco waters did not affect the 2001–2003 study area [*Del Vecchio and Subramaniam*, 2004].

[26] Monthly carbon uptake in the outer plume for conditions of mixing + biology (observed) and mixing-only (expected) were then calculated by multiplying the monthly plume surface area (Table 3) by the mean daily flux (based on climatological winds) and the number of days in the month. Because field observations in the plume were not available for all 12 months, we tried to match observed cruise S distributions with the climatologies. Sp03 fluxes represented May–June, Su01 fluxes were used for July–August, and F95 fluxes were applied to September–December. We used Sp96 data to represent the winter period (January–April) because the unusually low salinities observed east of the Amazon mouth that year (see Figure 1) generally correspond to conditions intermittently observed in February and March [*Geyer et al.*, 1996], when northerly winds impede along-shelf plume movement [see also *Nikiema et al.*, 2007].

3. Results

3.1. Observations

[27] Regions of low S (Figure 1), DIC, TA, and pCO_2 (Figure 2) extended north and northwest or northeast of the Amazon mouth for all cruises. In Sp03, DIC, TA, and pCO_2 were similar to those in other plume-influenced seasons [*Ternon et al.*, 2000; *Cooley and Yager*, 2006]. Minimum observed Sp03 DIC and TA values at S = 24.3 were 1457 and 1706 μmol kg^{-1}, respectively, 555–662 μmol kg^{-1} below mean seawater values (Figure 3). Surface pCO_2 in the southwesternmost study area fell as low as 201 μatm where S was lowest, and also exhibited lows in the moderate salinities of the mid- to northern study zone (Figures 1 and 2). Underway Sp03 pCO_2 was 201–402 μatm atm (mean = 337 ± 0.4, n = 10169), and underway SSS was 21.9–36.4 (mean = 33.5 ± 0.03, n = 10169). The Sp03 underway sea surface temperature (SST) ranged only from 26.3° to 28.6°C (mean = 27.7 ± 0.004°C; auxiliary Figure S1[1]). Low-carbon, low-S regions moved between seasons, but linear relationships between DIC or TA and S from 28 < S < 35 were highly conserved (r^2 = 0.827 and 0.997, respectively [*Ternon et al.*, 2000; *Cooley and Yager*, 2006]).

3.2. River Discharge Model

[28] The best regressions between discharge and precipitation climatologies (r^2 = 0.94 and 0.95 for GPCP and CMAP, respectively; auxiliary Figure S2) occurred with a 3 month lag between variables, consistent with the findings of *Zeng* [1999] for the Amazon. The climatology constructed from Óbidos gauge data (1979–1995) was correlated at r = 0.99 with *the Dai and Trenberth* [2002] climatology. The linear models coupling precipitation and discharge climatologies (CMAP and GPCP based) closely matched the projected discharge based on the Óbidos river gauge alone. The resultant discharge time series were correlated at r = 0.87 and 0.86 with the Óbidos data projected to the river mouth between 1979 and 1995. Linear models were also constructed on the basis of the relation between interannually varying precipitation and Óbidos data projected to the river mouth. The differences between precipitation-based and Óbidos-based discharge estimates were modest and indistinguish-

[1]Auxiliary materials are available in the HTML. doi:10.1029/2006GB002831.

Table 3. Plume Surface Area and Mean Monthly Plume CO_2 Uptake (±s.d.)

Month[a]	Surface Area, km^2	Uptake, Mixing Only, Gmol $month^{-1}$	Uptake, Mixing + Biology, Gmol $month^{-1}$
January	315,900	−9.1 ± 22.5	−4.5 ± 22.8
February	320,031	−8.3 ± 20.6	−4.2 ± 20.8
March	388,152	−11.1 ± 27.7	−5.6 ± 28.0
April	745,686	12.6 ± 49.1	176.8 ± 150.6
May	1,096,821	19.2 ± 74.6	268.7 ± 228.9
June	1,330,263	17.6 ± 65.0	207.8 ± 208.4
July	1,337,958	18.3 ± 67.6	216.0 ± 216.6
August	1,265,463	17.3 ± 63.9	204.3 ± 204.9
September	906,633	−17.7 ± 50.0	99.6 ± 103.9
October	507,384	−10.2 ± 28.9	57.6 ± 60.1
November	291,033	−5.7 ± 16.1	32.0 ± 33.4
December	268,434	−7.7 ± 19.1	−3.9 ± 19.4
Total, Gmol yr^{-1}		15.2 ± 162.8	1244.5 ± 474.3

[a]December–March uptakes were calculated from spring 1996 fluxes; April–May from spring 2003; June–August from summer 2001; September–November from fall 1995.

able between data sets and methods (rms = 0.6 or 11%). Relatively high correlation coefficients and low errors suggest that the method reasonably captured gross variability in the seasonal cycle associated with interannual climate patterns. Greater model error occurred at high precipitation and maximum discharge, where there is more scatter in the relationship (auxiliary Figure S2).

3.3. TA Prediction Model

[29] Andean discharge peaks in May and declines through the summer to its minimum in September (Figure 4a). The multiple regression equation relating TA_{Man} (Figure 4b) to Q_{Man} and A% was: TA_{Man} = 224.6(±69.23) + 5.981(±0.8435)*A% − 1.161 × 10^{-3}(±4.983 × 10^{-3})*Q_{Man}(±s.d., n = 74, r^2 = 0.42). The regression was significant, whereas relationships between TA_{Man} and other chemical or hydrographic variables were not [*Devol et al.*, 1995]. For the 25% of the data set withheld, predicted values ($Q_{Man,pred}$) were not significantly different from Hidroweb observations: $Q_{Man,pred}$ = 0.967 ± 0.033 (Q_{Man}) + 2612 ± 3305 (r^2 = 0.94, n = 53). As with Andean discharge, Q_{Total} also peaked in late spring (Figure 4c), but it showed a minimum in November. Discharge predictions made using the two models, CMAP and GPCP, were not significantly different from each other.

[30] Dilution-modeled interannual average monthly $TA_{Macapá}$ was 295 ± 61 μmol kg^{-1} (mean ± amplitude; Figure 4d), about a third lower than Óbidos values (360−600 μmol kg^{-1} [*Devol and Hedges*, 2001]). The bimodal pattern was a product of the May river discharge peak (Figures 4a and 4c) and the sinusoidal Andean TA supply (maxima in March and December, Figure 4b [*Devol et al.*, 1995]). Mixing-modeled average TA_r values from oceanic cruises (Figure 4d) nicely overlapped with interannual average values of dilution-modeled $TA_{Macapá}$ when

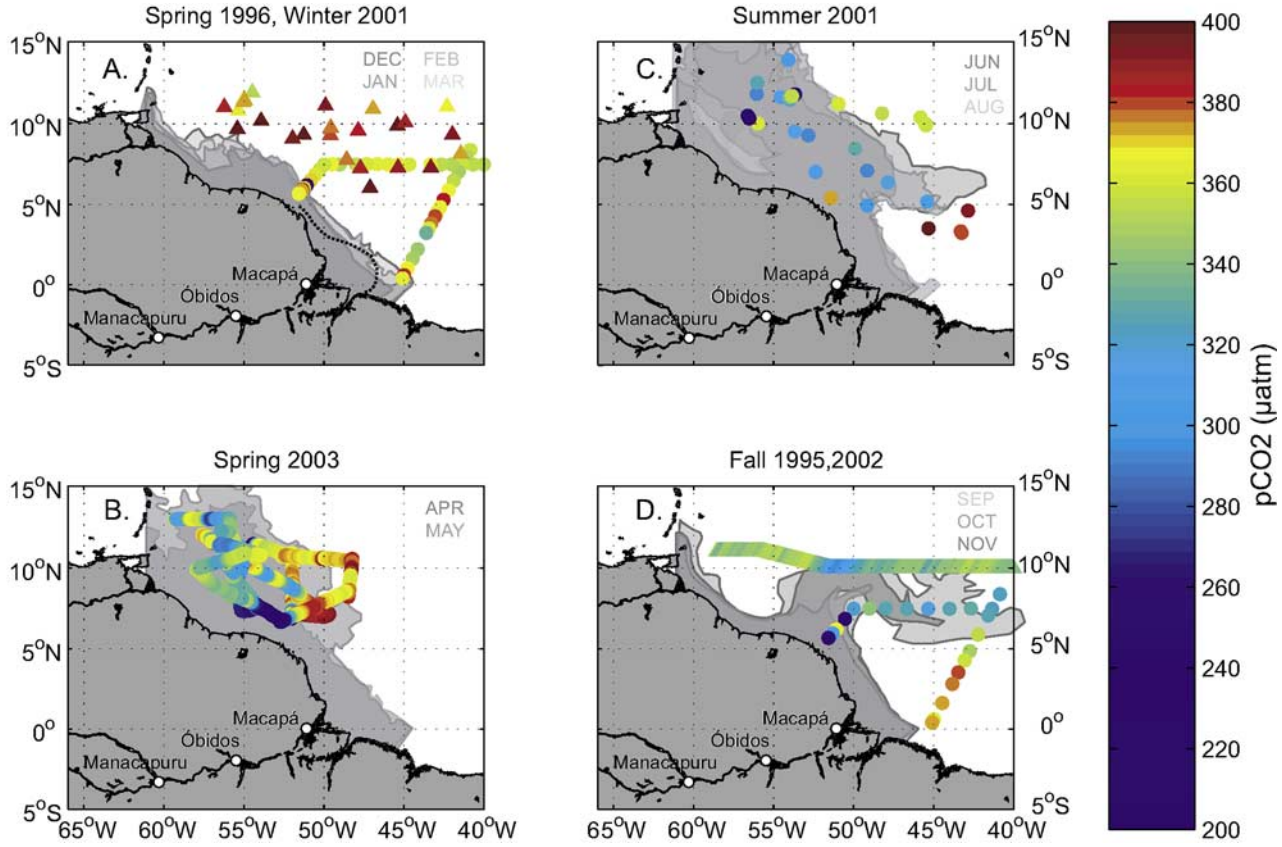

Figure 2. Sea surface pCO_2 (μatm) for each data set superimposed over monthly Amazon plume (S < 35) areas derived from satellite data. Seasons and cruises labeled as in Figure 1.

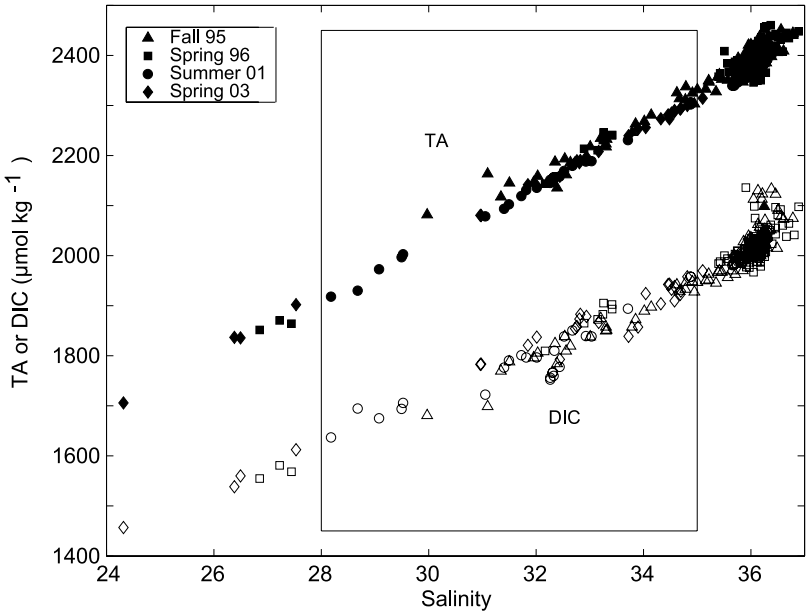

Figure 3. TA (solid symbols) and DIC (open symbols) plotted against salinity (S) for all data sets. Boxed data were used in the outer plume seasonal comparison. Oceanic samples had S > 35, whereas only spring samples included data below S = 28.

backed up by 1 month, allowing transit from the mouth. Modeled values also agree with historical data [*Gibbs*, 1972; *Stallard and Edmond*, 1983] during the spring and summer (Figure 4d), but are below measured values during the fall and winter when discharge is lowest. Our single measured 25 March 2002 Macapá TA hand sample (440.71 ± 0.37 μmol kg^{-1}; ±s.d., n = 2 at S = 0.0 ± 0.0, n = 3) was higher than the predicted April 2002 TA (353.5 μmol kg^{-1}; Figure 4d). After applying the TA = 0.82*DIC relationship to the Macapá DIC reported from November 1991 (363 μmol L-1 [*Druffel et al.*, 2005]), a TA of 298 μmol kg^{-1} was close to modeled $TA_{Macapá}$ (272 μmol kg^{-1}; Figure 4d), but significantly lower than observations from the 1960s [*Gibbs*, 1972]. Applying the 0.82 ratio to dilution-modeled TA predictions suggests yearly $DIC_{Macapá}$ was 360 ± 55 μmol kg^{-1} (mean ± amplitude), which agrees well with the few available observations [*Stallard and Edmond*, 1983; *Druffel et al.*, 2005].

[31] Interannual variability in Andean and total (Macapá) discharge (Figures 4a and 4c) related to precipitation and/or runoff caused small interannual variability in $TA_{Macapá}$ (Figure 4d). In 1991 and 1995, Andean discharge was significantly below the lower 95% confidence interval of the interannual average, and total river discharge was variable. This lower Andean discharge delivered less carbonate alkalinity to the main stem, and $TA_{Macapá}$ was at or below the 95% confidence interval. In 2001, Andean discharges were above the interannual average, but total main stem discharges were average, raising $TA_{Macapá}$ slightly above average levels.

3.4. Biological DIC Drawdown

[32] Observed variations in WTNA plume DIC not attributable to conservative mixing (ΔDICbio [*Cooley and Yager*, 2006]) averaged 26.1 ± 3.0 μmol C kg^{-1} for all seasons, with individual deficits up to 109 μmol C kg^{-1} (Figure 5a). A Model I linear regression [*Sokal and Rohlf*, 2000] of individual data plotted against day of year indicates no significant increase in ΔDIC_{bio} with time (r = 0.20, n = 76, p = 0.09). We did see a significant difference between cruises (Table 2; KW) due to the systematically lower Sp96 values. Mean seasonal values for ΔDIC_{bio} during Sp03, Su01, and F95 were not significantly different (p = 0.16) although data distributions varied (KW p = 0.05). There was no difference in ΔDIC_{bio} related to plume S groups (28–30, 30–32, 32–35). Since there was little seasonality in biological carbon drawdown within the 28 < S < 35 outer plume, any observed seasonal inorganic carbon changes must therefore be related to the size, shape, and location of the plume or plume phytoplankton community composition.

[33] As in Su01 [*Cooley and Yager*, 2006; Subramaniam et al., submitted manuscript, 2007], ΔDIC_{bio} was greatest in Sp03 at stations where *Richelia intracellularis/Hemiaulus hauckii* diatom-diazotroph assemblages (DDAs) were found. ΔDIC_{bio} at the surface correlated significantly with integrated *Richelia* abundance (r = 0.62, n = 57, p = 0.01). DDAs were observed in moderate S plume waters regardless of season (Subramaniam et al., submitted manuscript, 2007), so large ΔDIC_{bio} values in moderate-S, F95 plume waters suggest that DDAs may also have contributed to the biological carbon drawdown observed then. Other diazotrophs, such as *Trichodesmium*, did not show as large an impact on ΔDIC_{bio} in Sp03 or Su01 [*Cooley and Yager*, 2006].

3.5. Plume Uptake of CO_2

[34] Significant differences (p < 0.01) were observed among all cruises for solubility, observed and mixing-only

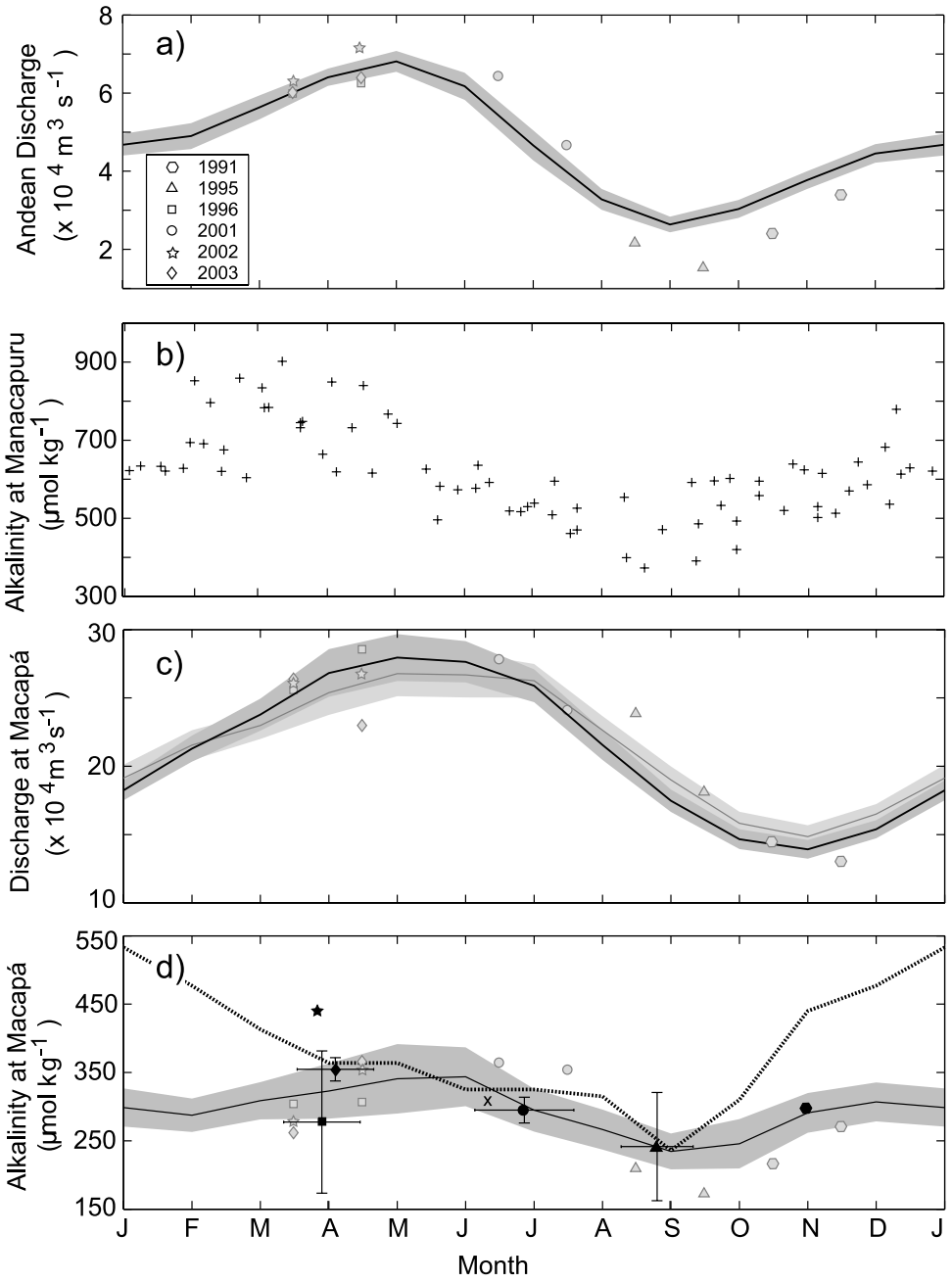

Figure 4. Dilution model input and results from Andes to Macapá; solid black lines plot interannual mean values, and gray shading shows 95% confidence intervals; solid gray symbols show data for specific years. (a) Monthly mean Andean discharge (10^4 m^3 s^{-1}; Sao Paulo de Olivenca) from Hidroweb. (b) Measured Manacapuru TA, January 1983 to November 1992, plotted over 1 year [adapted from *Devol et al.*, 1995]. (c) Monthly modeled mean Amazon total discharge (m^3 s^{-1}) adjusted to include precipitation using either the CMAP (black line, dark gray shading) or GPCP (gray line, light gray shading) data sets. (d). Modeled $TA_{Macapá}$ (Amazon mouth) calculated using CMAP derived total discharge (black line, dark gray shading). Black symbols (as in Figure 3) show mixing-modeled TA_r predictions from each cruise (ocean cruises moved forward one month to account for plume movement offshore) with vertical error bars showing 95% confidence intervals and horizontal error bars indicating the length of the cruise. The dashed line indicates Macapá data from 1963–1964 extracted from *Gibbs* [1972] using GraphClick (Arizona Software). The cross indicates near-mouth data from June 1976 [*Stallard and Edmond*, 1983].

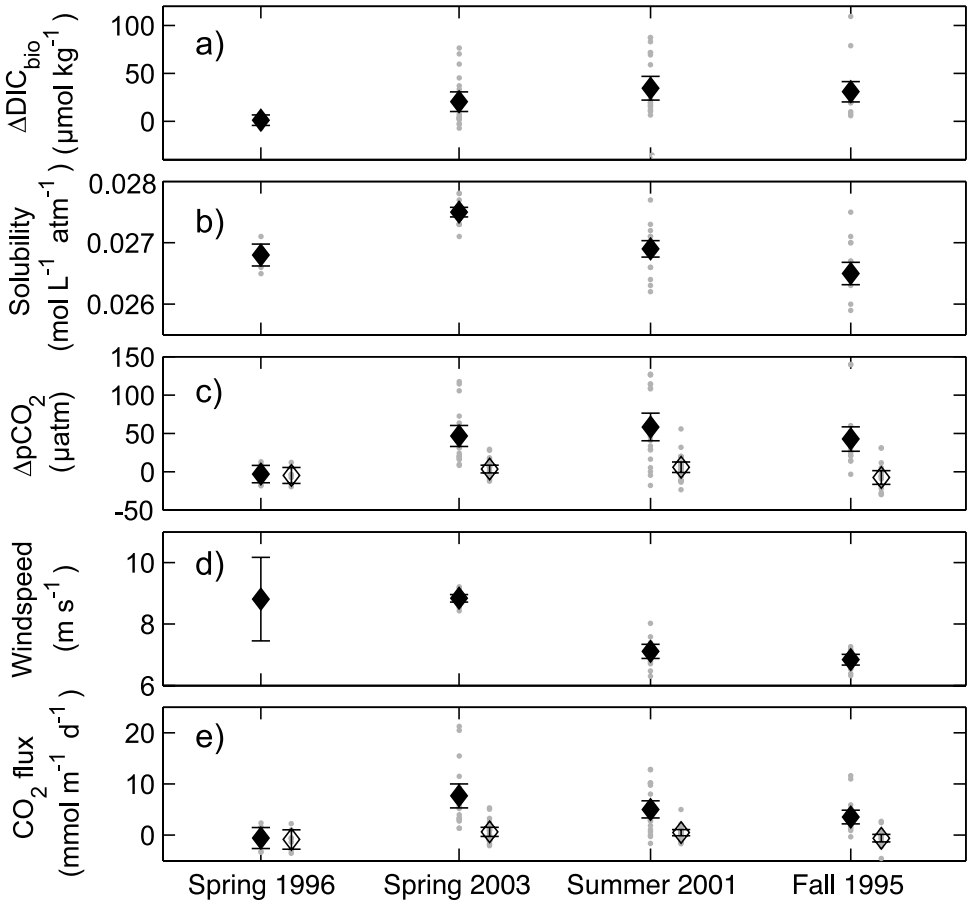

Figure 5. Data distributions (small gray dots) and mean values (large black diamonds with 95% confidence intervals shown) for 28 < S < 35 surface mixed layer samples from the four cruises. (a) ΔDIC_{bio} (μmol kg^{-1}); (b) CO_2 solubility (mol L^{-1} atm^{-1}) for observational data at in situ temperature and salinity; (c) air-sea pCO_2 gradient ($pCO_{2atm} - pCO_{2sea}$), for both mixing-only (open symbols) and observed/mixing plus biology (solid symbols); (d) Average wind speeds; and (e) calculated CO_2 flux rates for mixing-only (open symbols) or mixing plus biology/observed conditions (solid symbols). Positive fluxes indicate movement into the plume.

ΔpCO_2, climatological winds, and the observed and mixing-only CO_2 fluxes (Table 2). As with ΔDIC_{bio}, however, differences in ΔpCO_{2obs}, the gradient ($\Delta\Delta pCO_{2bio}$, the difference between ΔpCO_{2obs} and ΔpCO_{2mix}), and the flux attributable to biology ($\Delta Flux_{bio}$, the difference between $Flux_{obs}$ and $Flux_{mix}$) were due to the very different Sp96 data set (see Figure 5). Differences between Sp03, Su01, and F95 were not significant for ΔpCO_{2obs}, $\Delta\Delta pCO_{2bio}$, or $\Delta Flux_{bio}$ (Table 2). Significant differences were found only among S groups for ΔpCO_{2mix} and CO_2 $flux_{mix}$ (Table 2), suggesting that the biological impact was not sensitive to S at the level we grouped (28–30, 30–32, 32–35). Because we did not detect significant S-associated differences in most variables, mean values for each season are subsequently presented for the entire 28 < S < 35 zone.

[35] CO_2 solubility (Figure 5b and Table 2) was higher in Sp03 than in Su01 or F95 owing to cooler SST. Solubility during Sp03 was also higher than Sp96, which experienced anomalously warm SST related to Pacific-Atlantic atmospheric teleconnections [*Illig et al.*, 2006]. The overall temperature increase and solubility decrease from spring to fall caused seasons with similar ΔDIC_{bio} to have lower ΔpCO_{2obs} later in the year (Figure 5c and Table 3).

[36] Except during Sp96, values for cruise-averaged ΔpCO_{2obs} were positive ($pCO_{2atm} > pCO_{2sea}$; Figure 5c) and favored plume uptake from the atmosphere. The air-sea pCO_2 gradient expected from mixing only (ΔpCO_{2mix}) was near zero or slightly positive (Figure 5c), favoring very little CO_2 uptake in the outer plume. Climatological winds were highly seasonal (Figure 5d) and dropped by about 20% between spring and summer. Spring 1996 wind variability was likely related to the anomalous atmospheric conditions then [*Illig et al.*, 2006].

[37] Air-sea CO_2 fluxes calculated for observed conditions ($Flux_{obs}$, to which both mixing and biology contribute) were significantly higher than fluxes expected from mixing only ($Flux_{mix}$) in Sp03, Su01 and F95 by 4–7 mmol m^{-2} d^{-1} (Figure 5d). Although differences between observed and

predicted CO_2 fluxes varied somewhat across seasons (with a maximum in Sp03), the main difference was due to spring 1996 (Table 2). Available data does not indicate the exact cause of low spring 1996 ΔDIC_{bio}, which caused near zero $\Delta\Delta pCO_{2bio}$ and $\Delta Flux_{bio}$. Neither $\Delta\Delta pCO_{2bio}$ nor $\Delta Flux_{bio}$ differed significantly between Sp03, Su01, and F95 (Table 2 and Figures 5c and 5e). Observed fluxes were generally positive, indicating uptake within the $28 < S < 35$ zone (auxiliary material Figure S3). No S effect (Table 2) emerged for $Flux_{obs}$ or $\Delta Flux_{bio}$. Only $Flux_{mix}$ varied significantly with S. Without significant seasonal changes in biology, observed flux seasonality could be attributed entirely to solubility and wind speed decreases from spring to fall.

[38] When summed over the entire plume area across all seasons, biological activity enhanced the Amazon outer plume CO_2 sink by nearly 100x (Table 3). Under observed (mixing plus biology) conditions, the outer plume took up 1.245 ± 0.474 Tmol C yr^{-1} (15 ± 6 Tg yr^{-1}; Table 3). If mixing were the only influence, the outer plume would take up 0.015 ± 0.163 Tmol C yr^{-1} (0.2 ± 2 Tg yr^{-1}; mean $\pm$ s.d.), for a difference of $\sim$15 Tg C yr^{-1}.

4. Discussion

4.1. Conservative Versus Nonconservative Alkalinity Changes

[39] Because we know little about the carbonate system at the Amazon mouth, key assumptions of our analysis are that Andean runoff is the primary source of alkalinity to the main stem, that TA is dominated by carbonate alkalinity, and that TA travels conservatively through the lower main stem and offshore plume. Our models based on these ideas predicted TA at the river mouth by dilution ($TA_{Macapá}$) and offshore mixing (TA_r) with good agreement over the annual cycle (Figure 4d). Our models also agree well with some available data, including spring and summer 1963–1964 [*Gibbs*, 1972], summer 1976–1977 [*Stallard and Edmond*, 1983] values near the mouth, and the November 1991 Macapá hand sample [*Druffel et al.*, 2005] after applying the TA/DIC = 0.82 ratio [*Devol et al.*, 1995]. Agreement between seasonal Macapá TA patterns from both models (Figure 4d) suggests that plume TA seasonality can be explained largely by variations in basin drainage rather than by nonconservative behavior. Since most of the flux into the plume occurs between April and August, it is important to get the end-member right during those months.

[40] Some measurements indicate that river-mouth TA may be above our conservative model predictions, especially during winter. Our April 2002 Macapá hand sample TA was significantly higher than the dilution-model prediction (Figure 4d). This sample of opportunity may differ because it was handled differently from other samples, but storage conditions should have prevented carbonate alkalinity changes. Remineralization of noncarbonate ions such as ammonium and phosphate could have contributed somewhat to the higher measured TA value, but they could not raise TA the 100 μmol kg^{-1}. Historical bicarbonate data at the river mouth [*Gibbs*, 1972] (see Figure 4D) also suggests that fall and winter TA could be up to 250 μmol kg^{-1} higher than our predictions. The lack of a recent river mouth time series or winter plume data offshore hinders our ability to test this idea. Significant wintertime alkalinity contributions from lowland rivers could raise TA at the mouth above the prediction, but winter TA data for these tributaries are unavailable. Offshore carbonate-precipitating plankton could have caused us to underestimate river TA by as much as 28% of the maximum ΔDIC_{bio} (109 μmol kg^{-1}) or $\sim$30 μmol kg^{-1}, which is significant, but not enough to make the difference. Likely it is a combination of both factors. An increase in TA_r or DIC_r would similarly raise our estimates of NCP and biologically mediated gas exchange offshore.

[41] In any case, our analysis affirms that Macapá TA is likely well below the 600 μmol kg^{-1} estimate used in previous studies (TA_r = 600 μmol kg^{-1} and DIC_r = 600–744 μmol kg^{-1} [*Ternon et al.*, 2000; *Körtzinger*, 2003]) that set expected carbonate system mixing lines far above observed data. These studies explained the difference between mixing and observed regressions by invoking large production-related DIC losses from the early plume [*Ternon et al.*, 2000], possibly supplemented by carbonate equilibria shifts [*Körtzinger*, 2003]. DIC decreases owing to NCP are very likely [*DeMaster and Pope*, 1996; *DeMaster and Aller*, 2001], and apparent DIC deficits of 200 μmol kg^{-1} (almost twice the maximum of our outer plume ΔDIC_{bio}) can indeed be created on the continental shelf with observed inner-plume transit speeds and primary production rates [*Ternon et al.*, 2000]. Less likely are systematic plume TA decreases attributed to biological carbonate production off the shelf [*Ternon et al.*, 2000], because near-surface coccolithophorid abundance relative to other tropical Atlantic phytoplankton is quite low [*Aller and Aller*, 1986; *Kinkel et al.*, 2000] and they are not favored in the nearshore, high-nutrient zone, where diatoms thrive [*Iglesias-Rodriguez et al.*, 2002]. Neither coccolithophorids nor foraminifera were observed in the offshore plume during our cruises (E. J. Carpenter, personal communication, 2005). Along the entire plume-ocean mixing gradient, phosphate depletion implies that at least 96 μmol kg^{-1} DIC is biologically removed during transit [*Körtzinger*, 2003]. Our average NCP (26 ± 3 μmol kg^{-1}) for the outer 20% of the 0–36 S gradient is slightly higher than 20% of this phosphate-associated DIC removal. Thus the enhanced carbon drawdown due to biology calculated with our end-members is in line with biologists' observations and geochemists' predictions.

[42] Estimates of biological drawdown and flux calculations were also sensitive to our assumptions about the TA:DIC ratio at the river mouth [*Richey et al.*, 1991; *Ternon et al.*, 2000; *Cooley and Yager*, 2006]. Carbonate equilibria may shift when river and ocean water meet [*Körtzinger*, 2003], changing the TA:DIC ratio in the early plume, but the ratio is not likely to exceed 1 before S rises above zero. Given that the *Druffel et al.* [2005] DIC sample fits within our predicted TA range after applying the 0.82 ratio, the assumption seems reasonable until further data can be collected in the river mouth and early plume. Applying a ratio of 1, however, would bring it closer to the bicarbonate observations of *Gibbs* [1972]. The closer the TA:DIC ratio

of river water is to 1, the lower its pCO_2. If we had used a ratio of 1, our estimated mixing-only fluxes would be greater, decreasing by 30% the mean difference between mixing-only and mixing + biology fluxes from the current 4.8 ± 0.5 mmol C m^{-2} d^{-1} (n = 76) to 3.3 ± 0.5 mmol C m^{-2} d^{-1} (n = 76), and similarly decreasing our estimated annual biological enhancement of the Amazon plume carbon sink.

4.2. Seasonality in the Carbon Sink

[43] Inorganic carbon behavior along the river-sea continuum is influenced by both biological and physical processes, which vary enough in other estuarine and coastal systems to affect regional carbon source/sink status over an annual cycle [*Cai et al.*, 2003; *Frankignoulle and Borges*, 2001; *Thomas et al.*, 2004; *Tsunogai et al.*, 1999]. Seasonal variations in WTNA biological processes would affect the carbon sink by variably enhancing the air-sea pCO_2 gradient initially created by mixing, while changes in physical processes will influence gas transfer mechanics by changing piston velocity, solubility, or the amount of time surface water spends in contact with the atmosphere.

[44] We observed little ΔDIC_{bio} seasonality in the outer plume. The ΔDIC_{bio} reflects the instantaneous balance between NCP and air-sea replacement [*Cooley and Yager*, 2006]. Therefore ΔDIC_{bio} changes over time may result from a combination of change in both biology and gas exchange. Spring 2003 total primary production rates from outer plume stations (57 ± 7 mmol C m^{-2} d^{-1}, n = 29; D. Capone, personal communication, 2006) tended to be somewhat (∼15%) higher than but were not significantly different (T-test; p = 0.26) from Su01. Gas exchange rates slowed from spring to fall owing to solubility and wind speed changes, which would suggest that NCP slowed somewhat since ΔDIC_{bio} did not change significantly. High primary production rates year-round in the Amazon plume are likely supported by nitrogen fixation [*DeMaster and Aller*, 2001], and diazotroph species and abundance did not vary seasonally in the offshore plume (Subramaniam et al., submitted manuscript, 2007). Unfortunately, we have no primary production or community composition data from fall 1995 or spring 1996 to compare.

[45] Our annual calculation of plume uptake is less sensitive to our choice of which cruise's ΔDIC_{bio} applies to each month than it is to monthly plume areas and climatological conditions. Thus the most significant "biologically driven" seasonality we detected did not result from seasonal changes per square meter, but rather was caused by scaling biologically influenced fluxes up to the seasonally changing surface area of the plume. Since ΔDIC_{bio} varied little with S or season, conditions favorable to diazotroph-supported NCP must be linked to more complex processes, such as nutrient supply (Subramaniam et al., submitted manuscript, 2007), and more research is needed to understand these dynamics and their sensitivity to perturbation.

[46] Seasonal changes in TA_r and DIC_r within the dilution-modeled annual range would cause small changes in outer plume distribution, and therefore impact our calculations of the biological impact. The *Gibbs* [1972] data set raises the possibility that a large uncharacterized wintertime carbonate system shift may occur, greatly affecting this system. Our mixing model indicates that outer plume samples contain a small proportion of river water (average = 9% ± 0.5, n = 76). Increasing or decreasing mean TA_r and DIC_r by 2 standard deviations (±212 and ±259 μmol kg^{-1}, respectively; n = 76), for example, would increase or decrease plume TA_{exp} by an average of 0.7% (6 μmol kg^{-1}), and DIC_{exp} by 3.4% (59 μmol kg^{-1}). Increased DIC_{exp} would lead to a similarly greater ΔDIC_{bio}. The nearshore plume (S < 28), where we did not sample, contains a greater (>10%) proportion of river water. DIC changes due to river supply would therefore affect a larger proportion of a plume sample.

[47] Mixing affects plume DIC primarily by altering air-sea pCO_2 gradients. The vertical flux of CO_2 into the plume from underlying ocean water was assumed to be zero, because the strong pycnocline between them discourages vertical mixing and attenuates most of the normal upward carbon flux [*Cooley and Yager*, 2006; *Pailler et al.*, 1999; *Sprintall and Tomczak*, 1992]. In contrast, lateral mixing between river and ocean water dominates plume DIC distributions [*Cooley and Yager*, 2006] and causes a seaward decrease in both air-sea pCO_2 gradients and fluxes. In general, the plume moves quickly (0.54 m s^{-1}) from the river mouth to the retroflection zone (6°N) and slows thereafter (0.12 m s^{-1} [*Hellweger and Gordon*, 2002, and references therein]), with additional speed changes due to seasonal winds and currents [*Lentz*, 1995a]. Since WTNA air-sea CO_2 transfer (0–10 mmol C m^{-2} d^{-1}, Figure 5e) can lag biological production (2–30 mmol C m^{-2} d^{-1} [*Maranon et al.*, 2003]), the faster an individual water parcel travels from the Amazon mouth to the retroflection zone, lesser time is available for replacing DIC deficits. Faster plume speeds may enable a biologically induced carbon deficit to outlast the plume's physical structure. Low-S, low-pCO_2 zones extending to 25°W with no evidence of ongoing biological activity [*Lefevre et al.*, 1998; *Bakker et al.*, 1999] point to the far reach of plume effects.

4.3. Implications of Results on Carbon Sequestration

[48] Primary production based on nitrogen fixation is a key pathway for atmospheric carbon sequestration in the ocean [*Eppley and Peterson*, 1979]. Diazotrophy-associated production permits the offshore Amazon plume to take up significant quantities of atmospheric carbon. Under observed conditions that include positive NCP, the enhanced sink took up 15 ± 6 TgC yr^{-1}, which agrees well with estimates of diazotroph production in the plume (20.4 TgC yr^{-1}, calculated by rates of nitrogen fixation and a Redfield C:N ratio (Subramaniam et al., submitted manuscript, 2007)) and with sediment trap data suggesting a downward flux of 1.5–15 TgC yr^{-1} (Subramaniam et al., submitted manuscript, 2007)). Since our outer plume spanned a maximum surface area of 1.3 × 10^6 km^2, this corresponds to an average flux of 2.63 mmol C m^{-2} d^{-1}, which is nearly double the *Körtzinger* [2003] estimate of 1.33 mmol C m^{-2} d^{-1}. This result be partially due to our choices of end-members, but as a single transect, the *Körtzinger* [2003] estimate appeared less influenced by-productive patches. We believe sampling diazotroph-rich

waters in Sp03 and Su01 increased our mean flux estimates, given that DDA production (averaging 93 mmol C m^{-2} d^{-1} [*Carpenter et al.*, 1999]) is several times greater than open ocean primary production in the WTNA. Improved precision requires better knowledge of river end-members and better quantification of biological effects by sampling both irregular, patchy offshore blooms and inshore plume waters with $S < 28$ where production and respiration rates may be much higher.

4.4. Interannual Variability

[49] Our analysis begins to uncover interannual differences in WTNA inorganic carbon cycling. Spring 1996 data was collected during an anomalously warm period [*Illig et al.*, 2006], while F95 data was collected during a slightly negative phase (El Niño) of the Southern Oscillation Index (SOI; http://www.cpc.noaa.gov/products/precip/CWlink/MJO/enso.shtml). The other samples were collected during near-neutral periods. The western tropical North Atlantic SST remained near normal for most of 1995 and early 1996 [*Illig et al.*, 2006], likely driving normal moisture transport into the Amazon basin in the first months of 1996 (described by *Marengo and Nobre* [2001]) and leading to near-average Amazon discharge and predicted TA in the spring 1996 data sets (Figure 4). Anomalously warm spring 1996 conditions decreased solubility and increased wind speed variability (Figures 5b and 5d). Spring 1996 also appears to be a period during which NCP and the biological sink enhancement were minimal. Higher temperatures then may have triggered greater plume respiration or lower nutrient levels may have discouraged primary production.

[50] Future climate-driven changes influencing biological activity, meteorological conditions, or plume size will most affect the Amazon plume carbon sink. Unless the carbonate fraction of river TA changes significantly, variation in riverine TA or DIC will not likely change the sink offshore. Changes in river discharge or nutrient chemistry, however, may indirectly influence the offshore carbon sink through the biological community (Subramaniam et al., submitted manuscript, 2007). Drought in the Amazon basin, as in 2005, may be linked to rising western tropical North Atlantic SST [e.g., *Nobre and Shukla*, 1996]. Therefore global warming could decrease the Amazon plume carbon sink by shrinking plume surface area and decreasing the air-sea CO_2 gradient by reducing solubility. Enhanced blooms or export due to increased nitrogen fixation, biogenic silica generation, or grazing would increase ΔDIC_{bio}. Such changes would increase plume CO_2 uptake only if they occurred early in the year, when prevailing meteorological conditions enable sink uptake. That warmer spring 1996 conditions could have led to lower ΔDIC_{bio} values suggests that interannual changes can decrease biological sink enhancement according to local meteorological conditions. Alternatively, cooler or windier fall conditions, such as those in La Niña years [*Wang*, 2005], could increase total annual uptake by lowering plume pCO_2 and raise the air-sea transfer rate, promoting uptake for a longer period. Higher wind speeds may also encourage faster plume lateral mixing, reducing air-sea contact time and the air-sea CO_2 gradient, thereby countering some of the uptake due to a higher piston velocity.

5. Conclusion

[51] Although the WTNA is traditionally considered a CO_2 source to the atmosphere, biological activity in the Amazon plume permits uptake of an excess 15 ± 6 Tg C yr^{-1} from the atmosphere due to a combination of biological and physical controls. We examined both riverine and oceanic data to quantify biological and physical controls on plume inorganic carbon. By a seasonally changing combination of Andean carbonate dissolution and lowland dilution, the Amazon River delivers at least 295 ± 61 (mean ± amplitude) μmol kg^{-1} TA to the river mouth. Modeled alkalinities at the mouth agree very well with historical measurements made during the critical spring and summer months. Assuming DIC was supplied to the plume in proportion to TA, we quantify biological impacts on DIC offshore. Biological production, primarily associated with diatom-diazotroph assemblages (DDA), enables the offshore plume to take up CO_2 throughout the year at a rate (2.63 mmol C m^{-2} d^{-1}) nearly twice that previously reported in studies not likely encountering DDA-favoring conditions. Errors potentially associated with our assumptions about alkalinity would generally increase our estimates of biological production. Even so, our estimates of plume sink magnitude are within range of those determined with other methods [*Körtzinger*, 2003; *Ternon et al.*, 2000]. The apparent biological enhancement of the plume carbon sink is steady throughout the annual cycle, but air-sea CO_2 fluxes are heavily governed by physical factors. As a result, fall conditions are not as conducive to carbon sequestration as those in spring and summer. Changes in meteorological conditions (such as lower temperatures and higher wind speeds) during the fall would enhance plume uptake and have a greater impact on the sink than if they occurred in the spring or summer.

[52] **Acknowledgments.** This research was supported by the Office of Science (BER), U.S. Department of Energy, grant DE-FG02-02ER63472, NOAA Office of Global Programs grant NA16GP2689, and by faculty research support from the University of Georgia to P. L. Y. Financial support was provided to S. R. C. by the University of Georgia Presidential Graduate Fellowship and the NASA Earth System Science Fellowship. A. F. Michaels, D. G. Capone, and E. J. Carpenter graciously invited us into the MANTRA/PIRANA Biocomplexity Project, and with M. Neumann, shared data and provided excellent sampling access. S. Pluvinage assisted with sampling. B. Bergquist collected the Macapá hand sample. C. M. Tilburg assisted with sample analysis. C. E. Tilburg provided technical assistance on the Lanczos data filter. F. le Hingrat at IFREMER provided the ETAMBOT/SABORD data sets. A. Körtzinger kindly shared the Meteor 55 pCO_2 data.

References

Aller, J. Y., and R. C. Aller (1986), General characteristics of benthic faunas on the Amazon inner continental shelf with comparison to the shelf off the Changjiang River, East China Sea, *Cont. Shelf Res.*, *6*(1–2), 291–310.

Atlas, R., R. N. Hoffman, S. C. Bloom, J. C. Jusem, and J. Ardizzone (1996), A multi-year global surface wind velocity data set using SSM/I wind observations, *Bull. Am. Meteorol. Soc.*, *77*(5), 869–882.

Bakker, D. C. E., H. J. W. de Baar, and E. de Jong (1999), Dissolved carbon dioxide in tropical East Atlantic surface waters, *Phys. Chem. Earth, Part B*, *24*(5), 399–404.

Bates, N. R., A. F. Michaels, and A. H. Knap (1996), Seasonal and interannual variability of oceanic carbon dioxide species at the US JGOFS Bermuda Atlantic Time-series Study (BATS) site, *Deep Sea Res., Part II*, *43*, 347–383.

Bates, N. R., T. Takahashi, D. W. Chipman, and A. H. Knap (1998), Variability of pCO_2 on diel to seasonal timescales in the Sargasso Sea near Bermuda, *J. Geophys. Res.*, *103*(C8), 15,567–15,585.

Brainerd, K. E., and M. C. Gregg (1995), Surface mixed and mixing layer depths, *Deep Sea Res., Part I*, *42*, 1521–1543.

Broecker, W. S., and T. H. Peng (1982), *Tracers in the Sea*, Lamont-Doherty Geol. Obs., Palisades, N. Y.

Cai, W.-J., Z. A. Wang, and Y. Wang (2003), The role of marsh-dominated heterotrophic continental margins in transport of CO_2 between the atmosphere, the land-sea interface and the ocean, *Geophys. Res. Lett.*, *30*(16), 1849, doi:10.1029/2003GL017633.

Carpenter, E. J., J. P. Montoya, J. Burns, M. R. Mulholland, A. Subramaniam, and D. G. Capone (1999), Extensive bloom of a N_2- fixing diatom/cyanobacterial association in the tropical Atlantic Ocean, *Mar. Ecol. Prog. Ser.*, *185*, 273–283.

Cooley, S. R., and P. L. Yager (2006), Physical and biological contributions to the western tropical North Atlantic Ocean carbon sink formed by the Amazon River plume, *J. Geophys. Res.*, *111*, C08018, doi:10.1029/2005JC002954.

Dai, A., and K. E. Trenberth (2002), Estimates of freshwater discharge from continents: Latitudinal and seasonal variations, *J. Hydrometeorol.*, *3*, 660–687.

Del Vecchio, R., and A. Subramaniam (2004), Influence of the Amazon River on the surface optical properties of the western tropical North Atlantic Ocean, *J. Geophys. Res.*, *109*, C11001, doi:10.1029/2004JC002503.

DeMaster, D. J., and R. C. Aller (2001), Biogeochemical processes on the Amazon shelf: Changes in dissolved and particulate fluxes during river/ocean mixing, in *The Biogeochemistry of the Amazon Basin*, edited by M. E. McClain, R. L. Victoria, and J. E. Richey, pp. 328–357, Oxford Univ. Press, New York.

DeMaster, D. J., and R. H. Pope (1996), Nutrient dynamics in Amazon shelf waters—Results from AMASSEDS, *Cont. Shelf Res.*, *16*(3), 263–289.

DeMaster, D. J., W. O. Smith, D. M. Nelson, and J. Y. Aller (1996), Biogeochemical processes in Amazon shelf waters: Chemical distributions and uptake rates of silicon, carbon and nitrogen, *Cont. Shelf Res.*, *16*(5–6), 617–643.

Department of Energy (1997), Handbook of methods for the analysis of the various parameters of the carbon dioxide system in sea water, edited by A. G. Dickson and C. Goyet, *ORNL/CDIAC-74*, Washington, D. C.

Devol, A. H., and J. I. Hedges (2001), Organic matter and nutrients in the mainstem Amazon River, in *The Biogeochemistry of the Amazon Basin*, edited by M. E. McClain, R. L. Victoria, and J. E. Richey, pp. 275–306, Oxford Univ. Press, New York.

Devol, A. H., P. D. Quay, J. E. Richey, and L. A. Martinelli (1987), The role of gas exchange in the inorganic carbon, oxygen, and ^{222}Rn budgets of the Amazon River, *Limnol. Oceanogr.*, *32*(1), 235–248.

Devol, A. H., B. R. Forsberg, J. E. Richey, and T. P. Pimentel (1995), Seasonal variation in chemical distributions in the Amazon (Solimões) River: A multiyear time series, *Global Biogeochem. Cycles*, *9*(3), 307–328.

Dickson, A. G. (1981), An exact definition of total alkalinity and a procedure for the estimation of alkalinity and total inorganic carbon from titration data, *Deep Sea Res., Part A*, *28*, 609–623.

Dickson, A. G. (1990a), Standard potential of the reaction: $AgCl_{(s)} + 1/2\ H_{2(g)} = Ag_{(s)} + HCl_{(aq)}$, and the standard acidity constant of the ion $HSO_4^{(-)}$ in synthetic seawater from 273.15 to 318.15 K, *J. Chem. Thermodyn.*, *22*, 113–127.

Dickson, A. G. (1990b), Thermodynamics of the dissociation of boric acid in synthetic seawater from 273.15 to 318.15 K, *Deep Sea Res.*, *37*, 755–766.

Dickson, A. G., and F. J. Millero (1987), A comparison of the equilibrium constants for the dissociation of carbonic acid in seawater media, *Deep Sea Res., Part A*, *34*, 1733–1743.

Dickson, A. G., J. D. Afghan, and G. C. Anderson (2003), Reference materials for oceanic CO_2 analysis: A method for the certification of total alkalinity, *Mar. Chem.*, *80*, 185–197.

Druffel, E. R. M., J. E. Bauer, and S. Griffin (2005), Input of particulate organic and dissolved inorganic carbon from the Amazon to the Atlantic Ocean, *Geochem. Geophys. Geosyst.*, *6*, Q03009, doi:10.1029/2004GC000842.

Duchon, C. E. (1979), Lanczos filtering in one and two dimensions, *J. Appl. Meteorol.*, *18*, 1016–1022.

Edmond, J. M., E. A. Boyle, B. Grant, and R. F. Stallard (1981), The chemical mass balance in the Amazon plume: I. The nutrients, *Deep Sea Res., Part A*, *28*, 1339–1374.

Eppley, R. W., and B. J. Peterson (1979), Particulate organic matter flux and planktonic new production in the deep ocean, *Nature*, *282*, 677–680.

Frankignoulle, M., and A. V. Borges (2001), European continental shelf as a significant sink for atmospheric carbon dioxide, *Global Biogeochem. Cycles*, *15*(3), 569–576.

Geyer, W. R., R. C. Beardsley, S. J. Lentz, J. Candela, R. Limeburner, W. E. Johns, B. M. Castro, and I. D. Soares (1996), Physical oceanography of the Amazon shelf, *Cont. Shelf Res.*, *16*(5–6), 575–616.

Gibbs, R. J. (1972), Water chemistry of the Amazon River, *Geochim. Cosmochim. Acta*, *36*, 1061–1066.

Goyet, C., R. Adams, and G. Eischeid (1998), Observations of the CO_2 system properties in the tropical Atlantic Ocean, *Mar. Chem.*, *60*, 49–61.

Grimm, A. M. (2003), The El Niño impact on the summer monsoon in Brazil: regional processes versus remote influences, *J. Clim.*, *16*, 263–280.

Hellweger, F. L., and A. L. Gordon (2002), Tracing Amazon River water into the Caribbean Sea, *J. Mar. Res.*, *60*(4), 537–549.

Hood, R. R., et al. (2006), Pelagic functional group modeling: progress, challenges and prospects, *Deep Sea Res., Part II*, *53*, 459–512.

Huffman, G. J. (Ed.) (1997), The Global Precipitation Climatology Project monthly mean precipitation data set, report, 37 pp., World Meteorol. Organ., Geneva, Switzerland.

Iglesias-Rodriguez, M. D., C. W. Brown, S. C. Doney, J. A. Kleypas, D. Kolber, Z. S. Kolber, P. K. Hayes, and P. G. Falkowski (2002), Representing key phytoplankton functional groups in ocean carbon cycle models: Coccolithophorids, *Global Biogeochem. Cycles*, *16*(4), 1100, doi:10.1029/2001GB001454.

Illig, S., D. Gushschina, B. Dewitte, N. Ayoub, and Y. du Penhoat (2006), The 1996 equatorial Atlantic warm event: Origin and mechanisms, *Geophys. Res. Lett.*, *33*, L09701, doi:10.1029/2005GL025632.

Johnson, K. M., K. D. Wills, D. B. Butler, W. K. Johnson, and C. S. Wong (1993), Coulometric total carbon-dioxide analysis for marine studies: Maximizing the performance of an automated gas extraction system and coulometric detector, *Mar. Chem.*, *44*, 167–187.

Kinkel, H., K.-H. Baumann, and M. Cepek (2000), Coccolithophores in the equatorial Atlantic Ocean: Response to seasonal and Late Quaternary surface water variability, *Mar. Micropaleontol.*, *39*, 87–112.

Körtzinger, A. (2003), A significant CO_2 sink in the tropical Atlantic Ocean associated with the Amazon River plume, *Geophys. Res. Lett.*, *30*(24), 2287 doi:10.1029/2003GL018841.

Labat, D., J. Ronchail, J. Callede, J. L. Guyot, E. De Oliveira, and W. Guimaraes (2004), Wavelet analysis of Amazon hydrological regime variability, *Geophys. Res. Lett.*, *31*, L02501, doi:10.1029/2003GL018741.

Lee, K., F. J. Millero, and R. Wanninkhof (1997), The carbon dioxide system in the Atlantic Ocean, *J. Geophys. Res.*, *102*(C7), 15,693–15,707.

Lefevre, N., G. Moore, J. Aiken, A. Watson, D. Cooper, and R. Ling (1998), Variability of pCO_2 in the tropical Atlantic in 1995, *J. Geophys. Res.*, *103*(C3), 5623–5634.

Lentz, S. J. (1995a), The Amazon river plume during AMASSEDS: Subtidal current variability and the importance of wind forcing, *J. Geophys. Res.*, *100*(C2), 2377–2390.

Lentz, S. J. (1995b), Seasonal variations in the horizontal structure of the Amazon plume inferred from historical hydrographic data, *J. Geophys. Res.*, *100*(C2), 2391–2400.

Lentz, S. J., and R. Limeburner (1995), The Amazon River plume during AMASSEDS: Spatial characteristics and salinity variability, *J. Geophys. Res.*, *100*(C2), 2355–2375.

Lewis, E., and D. W. R. Wallace (1998), Program developed for CO_2 system calculations, version 1.05, *ORNL/CDIAC-105*, Carbon Dioxide Inf. Anal. Cent., Oak Ridge Natl. Lab., U.S. Dep. of Energy, Oak Ridge, Tenn.

Maranon, E., M. J. Behrenfeld, N. González, B. Mouriño, and M. V. Zubkov (2003), High variability of primary production in oligotrophic waters of the Atlantic Ocean: Uncoupling from phytoplankton biomass and size structure, *Mar. Ecol. Prog. Ser.*, *257*, 1–11.

Marengo, J. A., and C. A. Nobre (2001), General characteristics and variability of climate in the Amazon basin and its links to the global climate system, in *The Biogeochemistry of the Amazon Basin*, edited by C. R. McClain, R. L. Victoria, and J. E. Richey, pp. 17–41, Oxford Univ. Press, New York.

Marengo, J. A., B. Liebmann, V. E. Kousky, N. P. Filizola, and I. C. Wainer (2001), Onset and end of the rainy season in the Brazilian Amazon basin, *J. Clim.*, *14*, 833–852.

Mayorga, E., A. K. Aufdenkampe, C. A. Masiello, A. V. Krusche, J. I. Hedges, P. D. Quay, J. E. Richey, and T. A. Brown (2005), Young organic

matter as a source of carbon dioxide outgassing from Amazonian rivers, *Nature*, *436*, 538–541.

Mehrbach, C., C. H. Culberson, J. E. Hawley, and R. M. Pytkowicz (1973), Measurement of apparent dissociation constants of carbonic acid in seawater at atmospheric pressure, *Limnol. Oceanogr.*, *18*(6), 897–907.

Morel, F. M. M. (1983), *Principles of Aquatic Chemistry*, 446 pp., John Wiley, Hoboken, N. J.

Nikiema, O., J.-L. Devenon, and M. Baklouti (2007), Numerical modeling of the Amazon River plume, *Cont. Shelf Res.*, *27*, 873–899.

Nobre, P., and J. Shukla (1996), Variations of sea surface temperature, wind stress, and rainfall over the tropical Atlantic and South America, *J. Clim.*, *9*, 2464–2479.

Pailler, K., B. Bourles, and Y. Gouriou (1999), The barrier layer in the western tropical Atlantic Ocean, *Geophys. Res. Lett.*, *26*(14), 2069–2072.

Pätsch, J., W. Kühn, G. Radach, J. M. Santana Casiano, M. Gonzalez Davila, S. Neuer, T. Freudenthal, and O. Llinas (2002), Interannual variability of carbon fluxes at the North Atlantic Station ESTOC, *Deep Sea Res., Part II*, *49*, 253–288.

Quay, P. D., B. Tilbrook, and C. S. Wong (1992), Oceanic uptake of fossil fuel CO_2: Carbon-13 evidence, *Science*, *256*, 74–78.

Richey, J. E., J. I. Hedges, A. H. Devol, P. D. Quay, R. L. Victoria, L. A. Martinelli, and B. R. Forsberg (1990), Biogeochemistry of carbon in the Amazon River, *Limnol. Oceanogr.*, *35*(2), 352–371.

Richey, J. E., R. L. Victoria, E. Salati, and B. R. Forsberg (1991), The biogeochemistry of a major river system: The Amazon case study, in *Biogeochemistry of Major World Rivers*, edited by E. T. Degens, S. Kempe, and J. E. Richey, pp. 57–74, John Wiley, Hoboken, N. J.

Richey, J. E., J. M. Melack, A. K. Aufdenkampe, V. M. Ballester, and L. L. Hess (2002), Outgassing from Amazonian rivers and wetlands as a large tropical source of atmospheric CO_2, *Nature*, *416*, 617–620.

Rixen, T., C. Goyet, and V. Ittekkot (2006), Diatoms and their influence on the biologically mediated uptake of atmospheric CO_2 in the Arabian Sea upwelling system, *Biogeosciences*, *3*(1), 1–13.

Roy, R. N., L. N. Roy, K. M. Vogel, C. Porter-Moore, T. Pearson, C. E. good, F. J. Millero, and D. M. Campbell (1993), The dissociation constants of carbonic acid in seawater at salinities 5 to 45 and temperatures 0 to 45°C, *Mar. Chem.*, *44*, 249–267.

Sarmiento, J. L., R. Murnane, and C. LeQuere (1995), Air-sea CO_2 transfer and the carbon budget of the North Atlantic, *Philos. Trans. R. Soc., Ser. B*, *348*(1324), 211–219.

Smith, W. O., Jr., and D. J. DeMaster (1996), Phytoplankton biomass and productivity in the Amazon River plume: Correlation with seasonal river discharge, *Cont. Shelf Res.*, *16*(3), 291–319.

Sokal, R. R., and F. J. Rohlf (2000), *Biometry: The Principles and Practice of Statistics in Biological Research*, W. H. Freeman, New York.

Sprintall, J., and M. Tomczak (1992), Evidence of the barrier layer in the surface layer of the tropics, *J. Geophys. Res.*, *97*(C5), 7305–7316.

Stallard, R. F., and J. M. Edmond (1983), Geochemistry of the Amazon: 2. The influence of geology on the dissolved load at the time of peak discharge, *J. Geophys. Res.*, *88*(C14), 9671–9688.

Stumm, W., and J. J. Morgan (1996), *Aquatic Chemistry*, Wiley Intersci., Hoboken, N. J.

Sweeney, C., D. A. Hansell, C. A. Carlson, L. Codispoti, L. I. Gordon, J. Marra, F. J. Millero, W. O. Smith, and T. Takahashi (2000), Biogeochemical regimes, net community production and carbon export in the Ross Sea, Antarctica, *Deep Sea Res., Part II*, *47*, 3369–3394.

Takahashi, T., J. Olafsson, J. G. Goddard, D. W. Chipman, and S. C. Sutherland (1993), Seasonal variation of CO_2 and nutrients in the high-latitude surface oceans: A comparative study, *Global Biogeochem. Cycles*, *7*(4), 843–878.

Takahashi, T., R. A. Feely, R. F. Weiss, R. H. Wanninkhof, D. W. Chipman, S. C. Sutherland, and T. T. Takahashi (1997), Global air-sea flux of CO_2: An estimate based on measurements of sea-air pCO_2 difference, *Proc. Natl. Acad. Sci. U.S.A.*, *94*(16), 8292–8299.

Takahashi, T., et al. (2002), Global sea-air CO_2 flux based on climatological surface ocean pCO_2, and seasonal biological and temperature effects, *Deep Sea Res., Part II*, *49*, 1601–1622.

Ternon, J. F., C. Oudot, A. Dessier, and D. Diverres (2000), A seasonal tropical sink for atmospheric CO_2 in the Atlantic Ocean: The role of the Amazon River discharge, *Mar. Chem.*, *68*, 183–201.

Thomas, H., Y. Bozec, K. Elkalay, and H. J. W. de Baar (2004), Enhanced open ocean storage of CO_2 from shelf-sea pumping, *Science*, *304*, 1005–1008.

Tsunogai, S., S. Watanabe, and T. Sato (1999), Is there a "continental shelf pump" for the absorption of atmospheric CO_2?, *Tellus, Ser. B*, *51*(3), 701–712.

U.N. Educational, Scientific and Cultural Organization (1987), Thermodynamics of the carbon dioxide system in seawater: Report by the Carbon Dioxide Sub-Panel of the Joint Panel on Oceanographic Tables and Standards, *Tech. Pap. Mar. Sci. 51*, 45 pp., Paris.

Wang, C. (2005), ENSO, Atlantic climate variability, and the Walker and Hadley circulations, in *The Hadley Circulation: Present, Past and Future*, edited by H. F. Diaz and R. S. Bradley, pp. 173–202, Kluwer Acad., New York.

Wanninkhof, R., and W. R. McGillis (1999), A cubic relationship between air-sea CO_2 exchange and wind speed, *Geophys. Res. Lett.*, *26*(13), 1889–1892.

Weiss, R. F. (1974), Carbon dioxide in water and seawater: The solubility of a nonideal gas, *Mar. Chem.*, *2*, 203–215.

Xie, P. P., and P. A. Arkin (1997), Global precipitation: A 17-year monthly analysis based on gauge observations, satellite estimates, and numerical model outputs, *Bull. Am. Meteorol. Soc.*, *78*(11), 2539–2558.

Yager, P. L., D. W. R. Wallace, K. M. Johnson, W. O. Smith Jr., P. J. Minnett, and J. W. Deming (1995), The Northeast Water Polynya as an atmospheric CO_2 sink: A seasonal rectification hypothesis, *J. Geophys. Res.*, *100*(C3), 4389–4398.

Zeng, N. (1999), Seasonal cycle and interannual variability in the Amazon hydrologic cycle, *J. Geophys. Res.*, *104*(D8), 9097–9106.

V. J. Coles, University of Maryland Center for Environmental Science, Horn Point Laboratory, Cambridge, MD 21613, USA.

S. R. Cooley and P. L. Yager, School of Marine Programs, University of Georgia, Athens, GA 30602-3636, USA. (pyager@uga.edu)

A. Subramaniam, Lamont-Doherty Earth Observatory, Palisades, NY 10964-1000, USA.